Computational Methods
for Shell and Spatial Structures
IASS-IACM 2000
M. Papadrakakis, A. Samartin and E. Onate (Eds.)


# MODELLING OF BOUNDARY CONDITIONS FOR CYLINDRICAL STEEL STRUCTURES IN NATURAL WIND

**Thomas Ummenhofer**

IPP Ingenieursozietät Prof. Peil und Partner
Braunschweig, Germany
e-mail: ummenhofer@ipp-bs.de

**Peter Knoedel**

Vollack Stahltechnik GmbH & Co.
Karlsruhe, Germany
e-mail: pknoedel@vollack.de

**Key words:** Cylindrical Shell, Wind Loading; Boundary Conditions

**Abstract.** *This paper reports on wind loaded shell structures. The description of the wind pressure distribution around the shell circumference is discussed. Five different structural models to determine the relevant axial membrane stresses of wind loaded shells are presented. An example is presented for which the axial membrane stress distributions are calculated according to the given models. The results are compared and discussed.*

# 1 Introduction

Usually cylindrical shell structures such as tanks or steel stacks are fixed to the foundation by flanges with a certain number of anchor bolts, which are equally spaced along the bottom circumference. Since a rigid bottom ring is common practice, the structure is assumed to be continuously supported when determining the stresses in the shell wall and the anchor forces due to wind loads.

Depending on the geometry of the shell (R/T-ratio; L/R-ratio) the support reactions of the shell and the anchor forces can be determined by use of beam theory, or they have to be determined by shell theory. This is the case when under loading conditions cross sections remain not even, i.e. Bernoulli´s hypothesis is not valid.

Slender steel stacks can be modelled as cantilever beams since they have a big ratio of length to diameter. Special shells like for air condition buildings usually have a small ratio of length to diameter. The stress distribution in this compact shells under wind loading differs significantly from slender shells respectively beam theory. Some results of numerical studies on this problem have been published by Eibl/Curbach [1], Peil/Noelle [2] and Schneider/Thiele [3], [4].

Eibl/Curbach used a framework model to study the effects. Based on their results a formula has been established [5] which leads to a conservative limit of the applicability of beam theory.

$$\frac{L}{R} \geq 30 \cdot \log\left(\frac{R}{T}\right) - 10 \tag{1}$$

Where L is the shell length; T the thickness and R the radius of the shell.

A more accurate model was used by Peil/Noelle who used a FE-code to solve the problem. They established a criterion (2) which is picked up in the German steel stack code DIN 4133 [6]. The criterion defines when beam theory is still applicable to calculate the axial stresses.

$$\frac{L}{R} \geq 0.14 \cdot \frac{R}{T} + 10 \tag{2}$$

Since the criterion (2) was established with respect to estimate the maximum membrane compression stress to prevent shell buckling it is not applicable to get the maximum tension stresses for a pinned lower end of the shell. When the maximum compression stress reaches the value of the beam theory the tension stress may be underestimated by a factor of 2.3. Designing the anchor bolts of a shell the knowledge of the maximum tension stresses is essential.

An extensive numerical FE-parameter study was performed recently by Schneider/Thiele. The results are processed to multiply the cantilever beam solution by a factor k to get the shell theory results.

The formula provided is:

$$k = 0.50 + 2.94 \cdot \frac{R}{T} \cdot \left(\frac{R}{L}\right)^2 \tag{3}$$

Schneider and Thiele remark, that for values of k bigger than 4 the formula (3) is very conservative [7].

Different approaches concerning the modelling of the boundary conditions and their effect on the stress distribution in the shell are studied in the following.

An example of a real erected shell is used to quantify the effects of the different models.

## 2 Wind Loading

Applying the design wind load on a circular beam structure the resulting wind load per unit length is given by the product of the wind pressure and a force coefficient. Designing shells one has to remind that the wind pressure distribution around the circumference of a cylindrical shell is non uniform. It strongly depends upon Reynolds' number Re, which is defined in formula 4. But also the relation of the length of the shell to the diameter has an influence on the pressure distribution.

$$\mathrm{Re} = \frac{2R \cdot u}{\nu} \tag{4}$$

where u: is the wind speed and ν is the dynamic viscosity (~1,5*10$^{-5}$m²/s) of the air.

In the German code DIN 1055 part 4 [8] the wind pressure around the shell circumference is defined for three characteristical quantities of Reynolds' number. Values between this quantities may be interpolated logarithmically.

Figure 1 shows the pressure distribution according to the German standard.

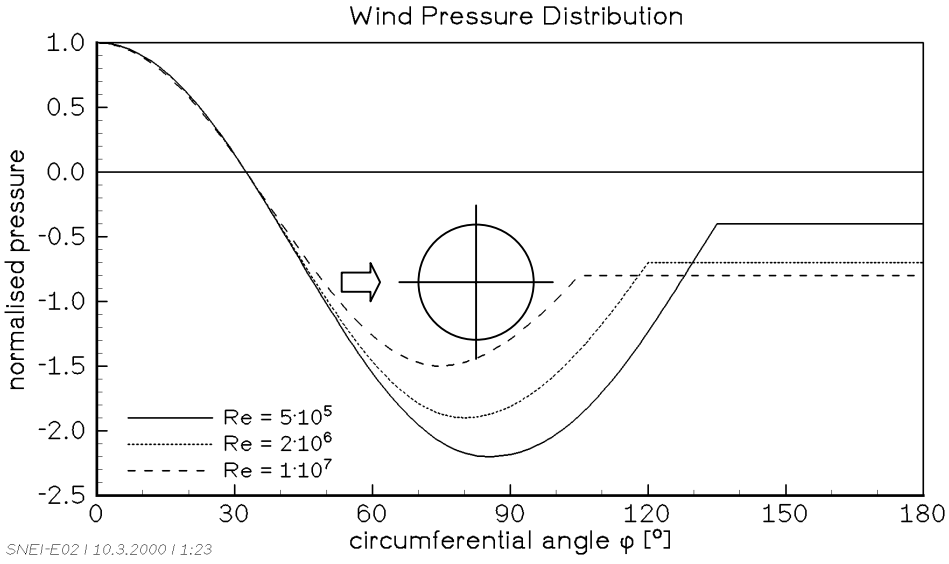


Figure 1: Wind pressure distribution according to DIN 1055 part 4

Unfortunately the code offers no formula to describe the curves in figure 1.

To enable an easy generation of the wind pressure distribution in a finite element model the function for Re ≈ $8 \cdot 10^7$ is divided in three sections. The curves in this sections are approached by quadratic functions of the form $w = ax^2 + bx + c$.

| | | | |
|---|---|---|---|
| Section 1 ($0° \le \varphi < 32°$): | a = -3.207; | b = 0; | c = +1.0 |
| Section 2 ($32° \le \varphi < 107.3°$): | a = +2.691; | b = -7.137, | c = +3.15 |
| Section 3 ($107.3° \le \varphi \le 180°$): | a = 0; | b = 0; | c = -0.78 |

It has be noted that Schneider/Thiele [4] also established best fit functions to describe the wind pressure distribution around the shell circumference according to DIN 1055 part 4.

For analytical purposes it is also possible to describe the wind loading by a Fourier series. Since only the lowest harmonics do have a significant influence on the results it is sufficient to model the characteristic pressure distribution by the first four or five Fourier coefficients.

In the investigations of Eibl/Curbach [1], Esslinger/Poblotzki [9] and Greiner [10] the coefficients of the Fourier function (5) are set like shown in table 1.

$$p_\varphi = \sum_{n=0,1\ldots4;5} (p_n \cdot \cos(n \cdot \varphi)) \tag{5}$$

| | **Fourier coefficients $p_n$ used by different authors** | | |
|---|---|---|---|
| N | Eibl/Curbach | Esslinger/Poblotzki | Greiner |
| 0 | -0.6440 | -0.8 | -0.55 |
| 1 | +0.2460 | +0.3 | +0.25 |
| 2 | +1.0340 | +1.4 | +0.75 |
| 3 | +0.5200 | +0.3 | +0.40 |
| 4 | -0.0956 | -0.2 | ±0.00 |
| 5 | -0.0421 | --- | -0.05 |

Table 1: Comparison of Fourier coefficients for wind pressure distribution

A comparison of the above listed functions is given in figure 2. It is obvious that the graph based on the quadratic functions represents the curve given in the DIN 1055 part 4 for Reynolds' numbers Re higher than $10^7$.

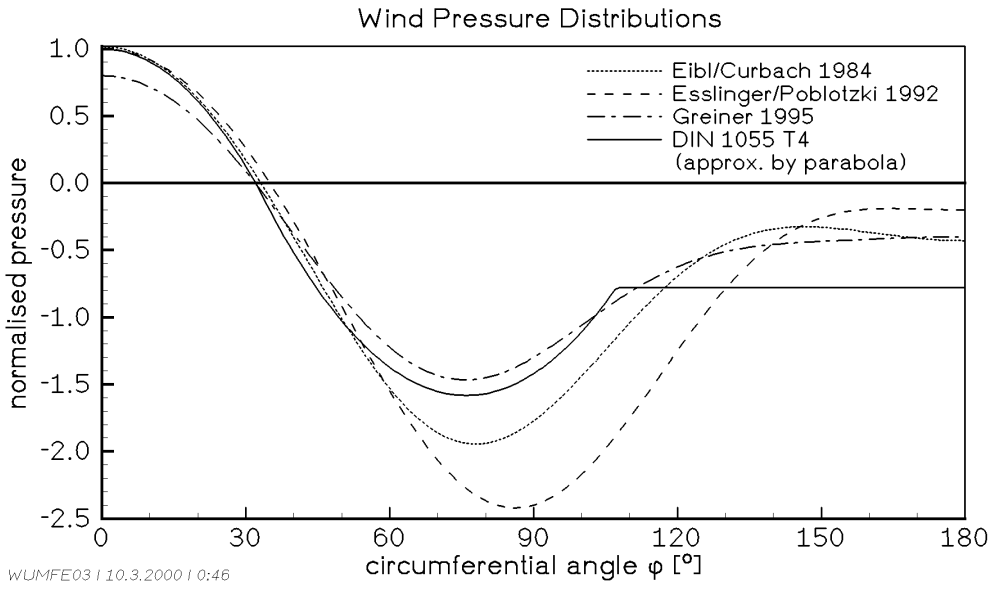


Figure 2: Comparison of different approximations for the wind pressure distribution

## 3 Structural Models

Five different models are presented in the following which can be used to calculate the maximum axial shell membrane stresses. With increasing number the models get closer to the real structural behaviour. The method of solution required for the five different models is listed in table 2.

| Model | Method of solution required |
|---|---|
| Model 1: clamped beam | analytical, simple |
| Model 2a: membrane shell | analytical, 1 to 5 Fourier harmonics |
| Model 2b: membrane shell | FE-code, "real" pressure distribution |
| Model 3a: shell, bottom flange modelled by springs | axisymmetric shell code with non-axisymmetric loading or 3-D code |
| Model 3b: shell with bottom flange | axisymmetric shell code with non-axisymmetric loading or 3-D code |
| Model 4: shell with bottom flange, uni-lateral contact, smeared anchor bolt stiffness | FE-code nonlinear, 3-D, contact-elements |
| Model 5: shell with bottom flange, uni-lateral contact, discrete elastic anchor bolts | FE-code 3-D nonlinear, contact-elements |

Table 2: Structural models and methods of solution required

### 3.1 Model 1: beam theory

When modelling the shell structure as a cantilever beam, along-wind loads are considered only. The clamping moment is calculated by the known formula of beam theory, the stresses by use of Bernoulli´s hypothesis. This gives the known cosine-distribution of the longitudinal stresses along the circumference.

The maximum stresses neglecting the normal stresses due to dead load can be calculated by

$$\sigma_{\max} = \pm \frac{q_0 \cdot L^2}{\pi \cdot R \cdot T} . \tag{6}$$

### 3.2 Model 2: membrane shell

#### 3.2.1 Model 2a: analytical, one Fourier-coefficient

With thin walled and non-slender shells beam theory does not yield proper results for the bottom forces of the structure. Because of the non-uniform distribution of the wind pressure along the circumference of the shell the membrane forces at the bottom are different from the above cosine-distribution.
Using shell membrane theory with suppressed vertical displacements at the bottom edge gives meridional membrane forces, which can extent the results of beam theory by a factor of five with common structures.

Using the equations of Greiner's semi-membrane theory [11] the maximum stresses in the shell are given by the following equation (7) in dependence of the wave number N.

$$\sigma_x = \sum_{n=0,1..4;5} \frac{p_N \cdot L^2}{8 \cdot R \cdot T} \cdot N^2 \tag{7}$$

This holds for shells where:

$$\left(\frac{L}{R}\right)^2 \cdot \frac{T}{R} \cdot \frac{N^2}{4} \cdot (N^2 - 1) \le 1 \tag{8}$$

For engineering purposes it is sufficient to solve equation (7) only for the dominating Fourier coefficient. Since the wind suction on the sides of the cylinder, which deforms the cylindrical shell is the dominating influence, equation (7) is solved for N = 2 (cos2φ-distribution). According to figure 1 $p_{N=2}$ has a value between 1.5 and 2.2, depending on Reynolds' number.

#### 3.2.2 Model 2b: analytical/numerical by FE-code

Based on a membrane theory the shell stresses are calculated numerical. The pressure distribution along the circumference is considered as given in figure 1. The bottom flange is not modelled. At the lower end the shell is assumed to be pinned which means that $u_x$, $u_y$ and $u_z$ are set to zero.

### 3.3 Model 3: shell with bottom flange

#### 3.3.1 Model 3a: flexural stiffness of flange is accounted for by springs

The above shell model can be improved by introducing a continuous elastic support along the bottom edge into the finite element model, which accounts for the flexural stiffness of the bottom flange. The elastic rotational spring stiffness of the flange is modelled by springs.

The modulus of the support has to be estimated by determination of the flexural stiffness of a plain slice of the bent bottom flange, which is a shortcoming of this alternative model.

#### 3.3.2 Model 3b: flange dimensions modelled in FE-model

A further improvement is gained by modelling the geometry of the bottom flange. This can be done by an axisymmetric shell code which can handle non-axisymmetric loading or by an 3-D code. The lower flange is accounted for by taking its real dimensions into the numerical model. In this case the stiffness of the bottom flange results from material parameters.

The structure is supported continuously along the anchor circle. The three displacements $u_x$, $u_y$ and $u_z$ are set to zero. This model accounts for the flexibility of the flange. The peak forces at the bottom are reduced, since the bottom cross section of the shell can rather deform as predicted by Bernoulli´s hypothesis.

### 3.4 Model 4: shell with bottom flange, smeared anchor bolt stiffness, unilateral contact

The model is improved by taking into account the distributed elastic anchor bolts stiffness. The nodes lying on the circle anchor bolts are elastically fixed by spring elements, the stiffness of which is chosen to fit the stiffness of real discretely set anchor bolts, so only the axial stiffness of the anchor bolt has to be assumed. The contact and possible gap between bottom flange and concrete base is accounted for by nonlinear contact elements. Prestressed anchor bolts may be considered.

### 3.5 Model 5: shell with bottom flange, unilateral contact, discrete anchor bolts

A further refinement of the model can be made by introducing the discrete anchor bolt location around the circumference of the flange into the model. Prestressing of the anchor bolts may be included. The distance between the anchor bolts has a strong influence on the local stiffness of the bottom flange and may lead to considerable stress peaks if it is to large. This effect influences the stress distribution locally but not globally. Therefore this model will not be considered in the following example.

## 4 Example

A numerical study on the effects of the different models on the calculated maximum membrane stresses in axial direction was performed. For the FE-models the finite element code ANSYS 5.6 was used.

The shell was modelled by shell elements STIFF43, the anchors by spring elements COMBIN 14. With model 4 every node in the middle span of the bottom flange was fixed by an elastic spring with a spring stiffness of k = 1 kN/mm. Prestressing of anchor bolts was not considered. For the simulation of the contact area between shell and concrete base contact elements CONTAC113 were used. Due to symmetry the numerical model described only one half of the shell. At the nodes of the symmetry edges symmetrical boundary conditions were applied. In circumferential direction 60 and in vertical direction 180 elements were chosen. The wind pressure distribution around the circumference was generated like shown in chapter 2 for Re $\approx 8 \cdot 10^7$. This may lead to slightly non conservative results for the stresses, since Reynolds' number for the structure with the below dimensions would be only Re $\approx 5.3 \cdot 10^7$.

**Geometry:**

R = 1000 mm

L = 5000 mm R/T = 333

T = 3 mm L/R = 5

upper flange 5 x 60 mm

bottom flange 5 x 200 mm

$I = \pi \cdot R^3 \cdot T = 9.42 \text{ x } 10^9 \text{ mm}^4$

$W = I/R = 9.42 \cdot 10^6 \text{ mm}^3$

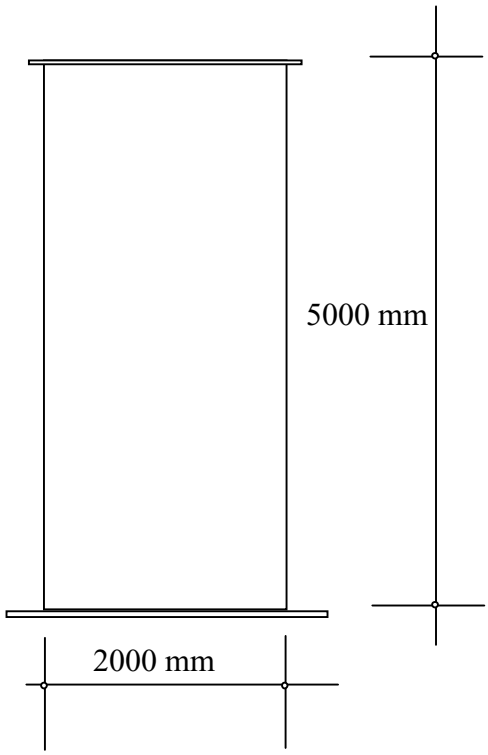


**Material:**

E = 170.000 N/mm² (stainless steel; $f_{y0}$ = 195 N/mm²)

**Wind load:**

$Re = 2 \cdot 40.0/1.5 \cdot 10^{-5} = 5.33 \text{ x } 10^6$

Design wind velocity v = 40 m/s

wind pressure $q_0$=1.0 kN/m²

reduction coefficient $\psi$ = 0.64 (DIN 1055 part4)

compression coefficient at $\varphi = 0°$ $c_{p0} = 1$

compression coefficient at $\varphi = 0°$ $c_{p0min} = -1.5$

integration coefficient $c_{f0}$ = 0.75 (DIN 1055 part 4)

**Beam theory:**

max. $M = q_0 \cdot \psi \cdot c_{f0} \cdot 2 \cdot R \cdot L^2/2 = 12.0$ kNm

criterion eqn (2): $0.14 \cdot R/T + 10 = 56.6 > L/R = 5 \Rightarrow$ beam theory not applicable

$\sigma_{beam}$ = 1.27 N/mm² ; eq.6 (stresses due to dead load of structure are neglected)

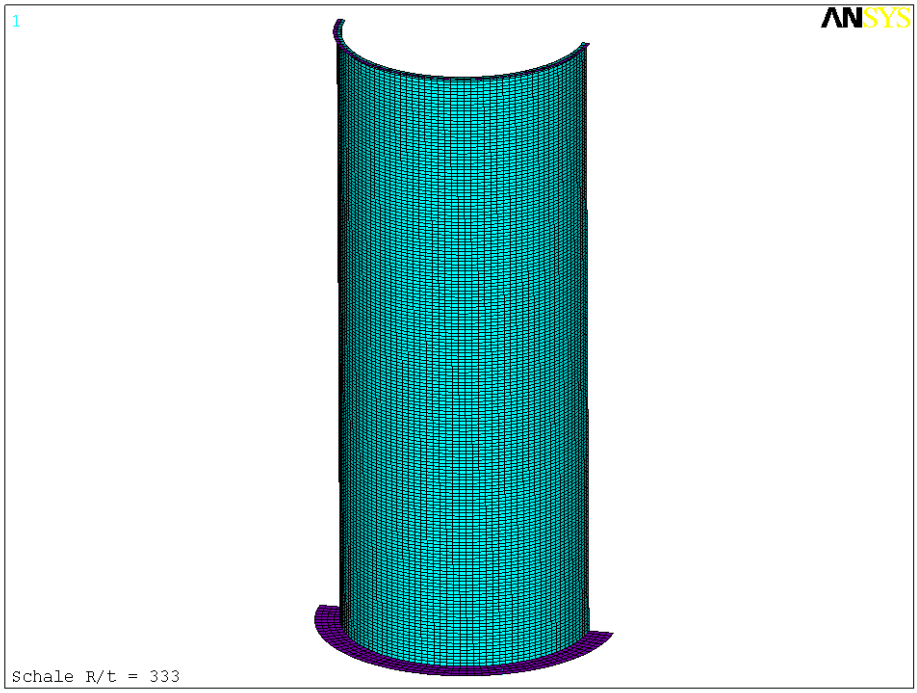


Figure 3: Element mesh

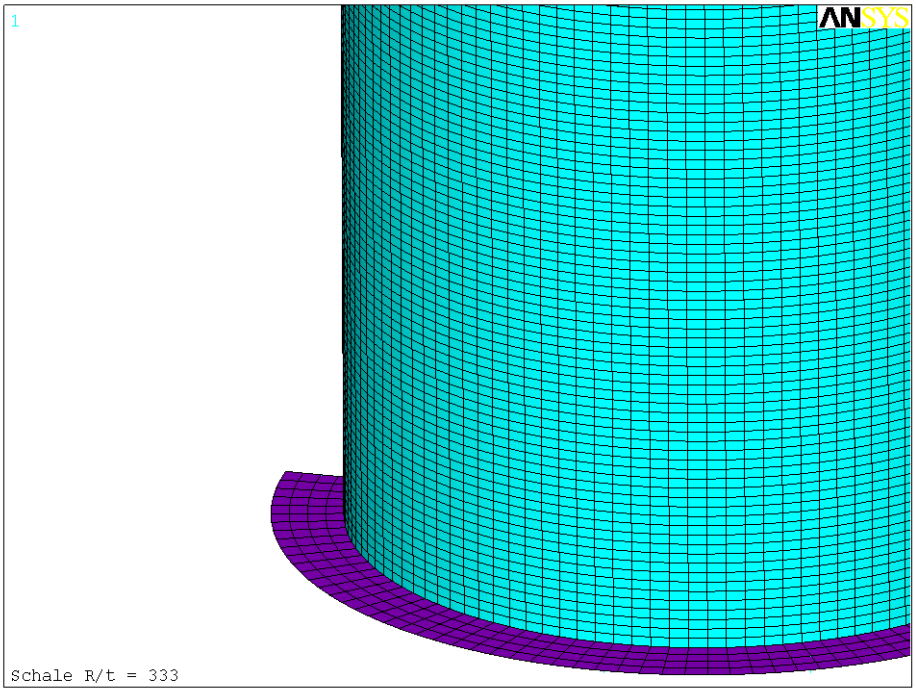


Figure 4: Meshing of bottom area

Figure 3 and 4 are showing the element mesh used for the FE-analyses.

In table 3 dimensionless axial stresses in the bottom area of the shell are listed. The calculated results are normalised by the beam stress $\sigma_{beam}$ according to equation (6), which means that the actual maximum stress is divided by the beam stress.

| | **maximum axial dimensionless membrane stresses** | |
|---|---|---|
| **Model** | compression min $\sigma_x/\sigma_{beam}$ | tension max $\sigma_x/\sigma_{beam}$ |
| model 1: beam theory | 1.00 | 1.00 |
| model 2a: membrane shell, 2nd Fourier-coefficient set to 2) | 6.56 | 6.56 |
| model 2b: membrane shell, "real" wind pressure | 7.20 | 10.00 |
| model 3b: shell with bottom flange | 0.69 | 1.24 |
| model 4 : shell with bottom flange, unilateral contact, smeared anchor bolt stiffness | 2.82 | 1.44 |

Table 3: Comparison of calculated maximum axial membrane stresses at lower end of shell

The results show the significant influence of the model used on the calculated stresses. If it is kept in mind that the model 4 is closest to reality it can be stated, that both models 2a and 2b lead to a strong overestimation of the real stresses in the bottom area. Because of the 'soft' boundary conditions the use of model 3b results in an underestimation of the stiffness of the bottom area. The stresses calculated with this model are too low.

The following figures 5 to 11 show axial stress distributions and displacements for the computed models 2b, 3b and 4. In the figures the deformed structure is plotted by an amplification factor of 50.

In figure 7 ff. the deformation of the bottom flange is obvious. Figure 11 also shows the contact area below the flange. The green lines indicate the spring elements.

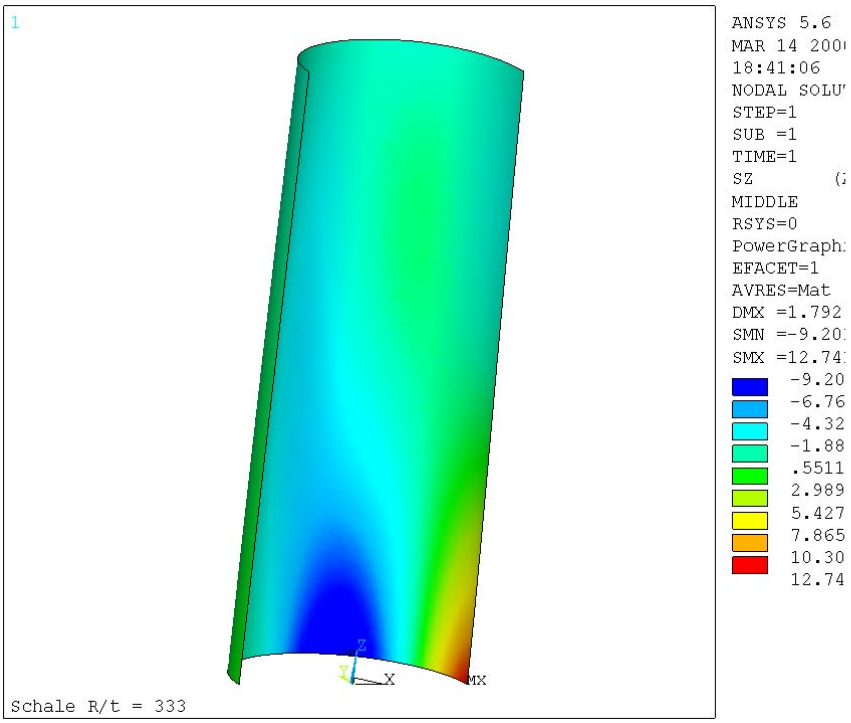


Figure 5: Axial stress distribution for model 2b [N/mm²]

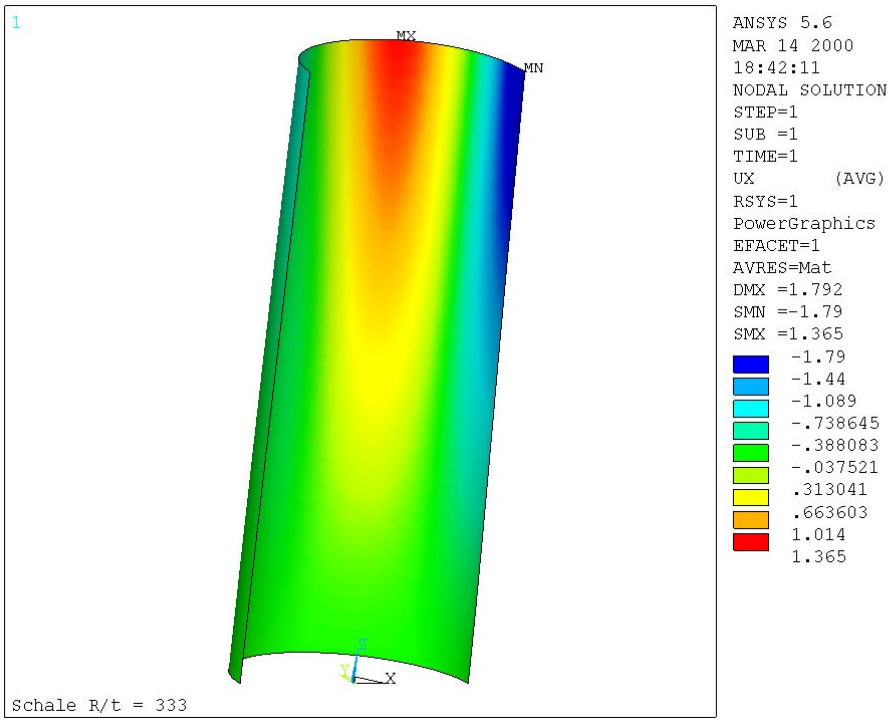


Figure 6: Radial displacements for model 2b [mm]

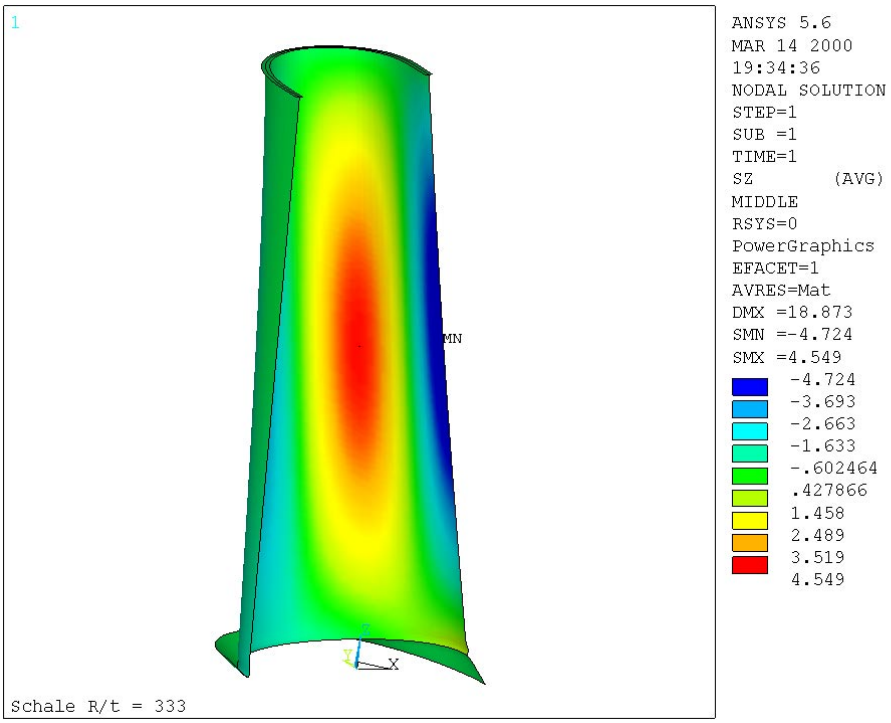


Figure 7: Axial stress distribution for model 3b [N/mm²]

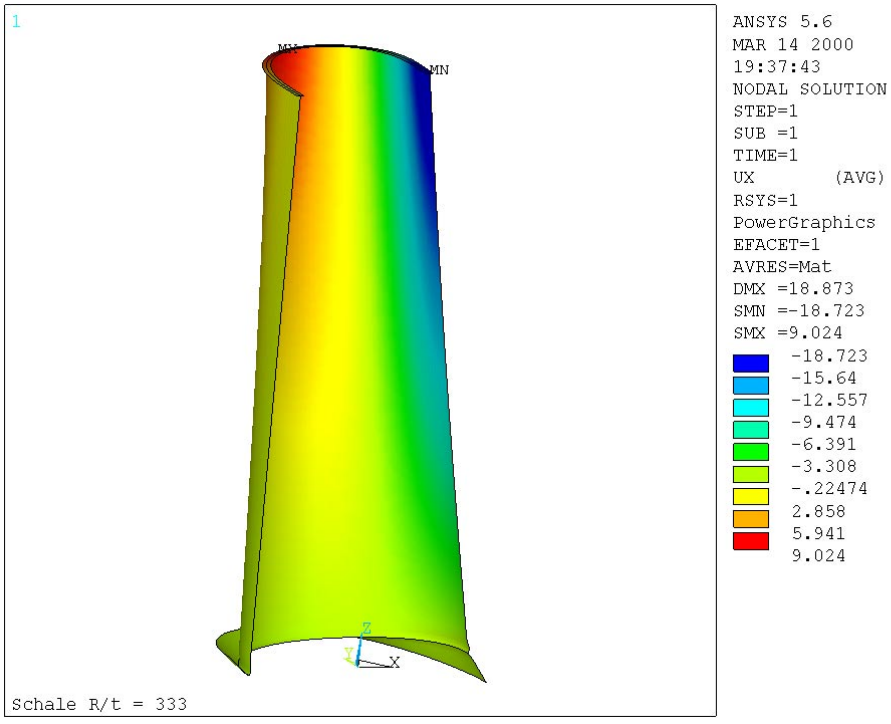


Figure 8: Radial displacements for model 3b [mm]

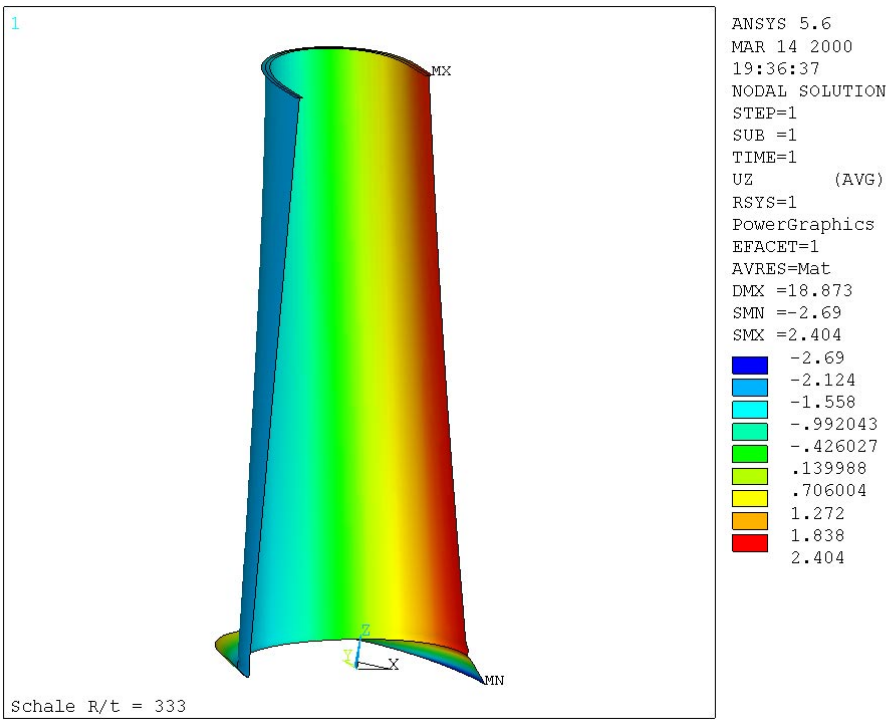


Figure 9: Axial displacements for model 3b [mm]

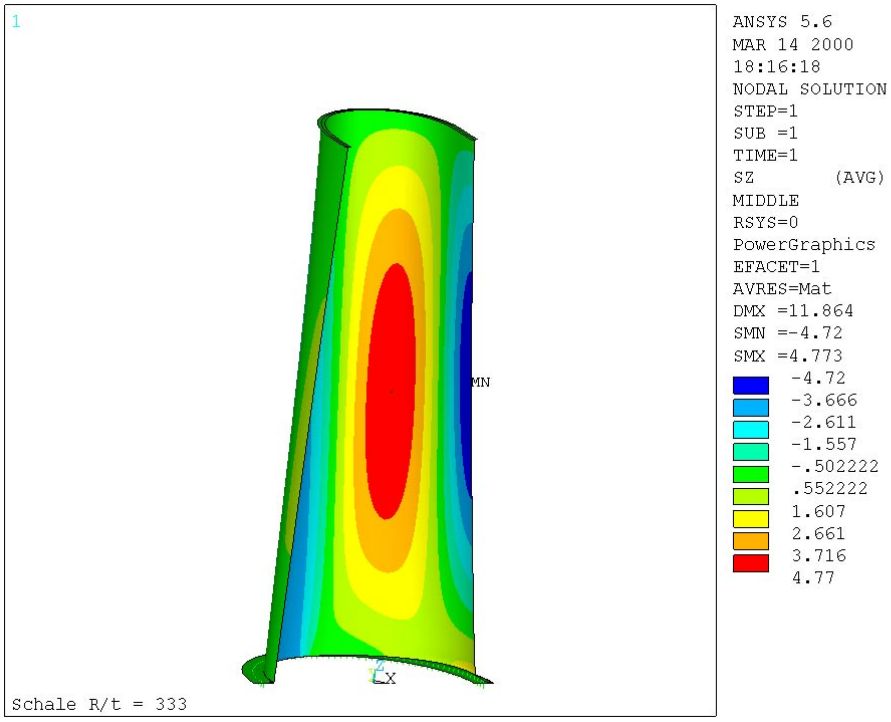


Figure 10: Axial stress distribution for model 4 [N/mm²]

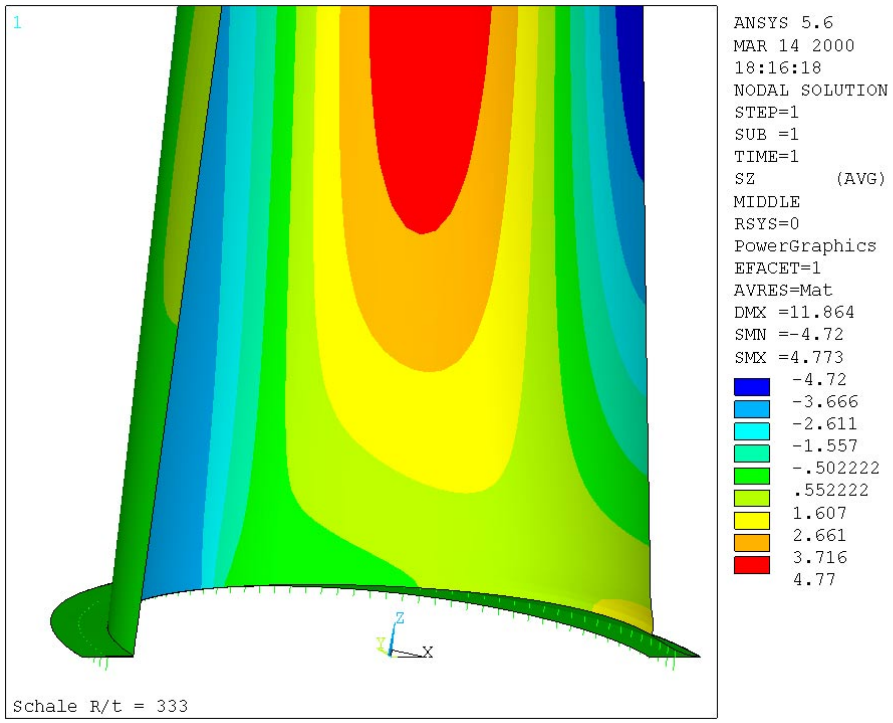


Figure 11: Axial stress distribution at bottom of shell for model 4 [N/mm²]

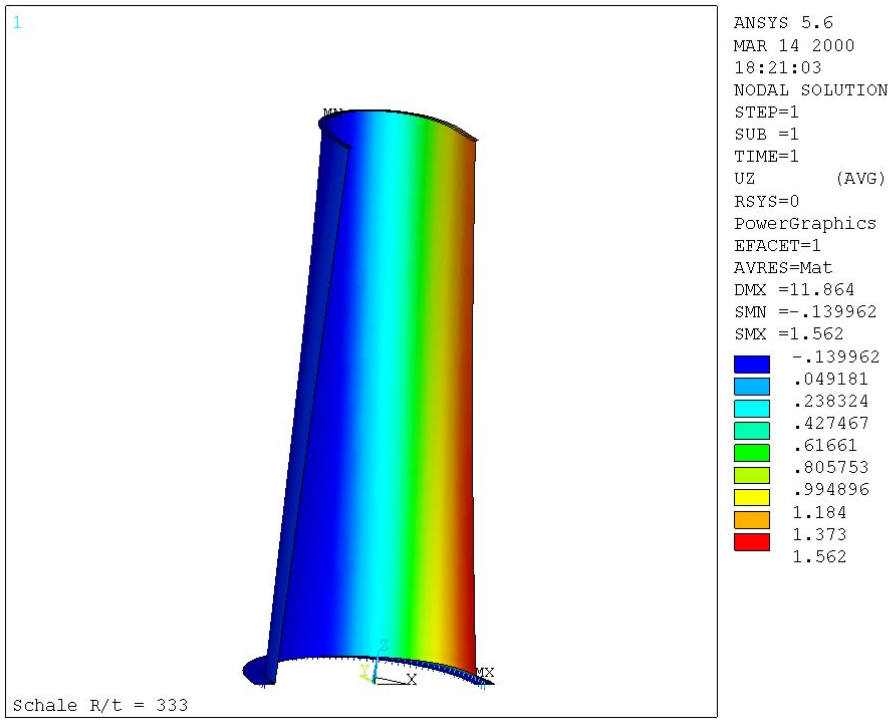


Figure 12: Axial displacements for model 4 [mm]

## 5 Conclusions

The results of this study show that the modelling of the boundary conditions of the shell has a significant influence on the resulting maximum axial shell membrane stresses at the bottom flange. This is of interest for the design against axial buckling of the shell and as well for the design of the bottom flange dimensions and the anchor bolts.

Beam theory may lead to a strong underestimation especially of the compression stresses. Shell theory with pinned ends leads to very conservative results. Since the elastic behaviour of the bottom flange may extremely reduce the axial tensile stresses, this can be advantageous concerning the necessary anchor dimensions.

## References

[1] J. Eibl, M. Curbach, *Randschnittkräfte auskragender zylindrischer Bauwerke unter Windlast,* Bautechnik 61 (1984) 275-279.

[2] U. Peil, H. Noelle, *Zur Frage der Schalenwirkung bei dünnwandigen zylindrischen Stahlschornsteinen,* Bauingenieur 63 (1988) 51-56.

[3] W. Schneider, R. Thiele., *The stress and strain state in the base of wind-loaded steel chimneys,* In Proc. 5th Int. Conf. Offshore and Polar Engineering ISOPE, The Hague, The Netherlands (1995) 104-108.

[4] W. Schneider, R. Thiele., *Schnittkraftverteilung im Fußbereich stählerner Schornsteine*, In Proc. *Schornsteinbau-Symposium Bad Hersfeld*, VSA, Pforzheim, Germany (1998).

[5] C. Petersen, *Stahlbau,* Vieweg-Verlag, Berlin (1993).

[6] DIN 4133, *Steel stacks,* Beuth-Verlag, Berlin (1991).

[7] W. Schneider, private communication to P. Knoedel, (1998).

[8] DIN 1055 Part 4, *Design loads for buildings, wind loads on structures not susceptible to vibrations,* Beuth Verlag, Berlin (1986).

[9] M. Esslinger, G. Poblotzki, *Buckling under wind loading* (in German*),* Stahlbau 61 (1992) 21-26.

[10] R. Greiner, *Cylindrical shells: wind loading,* In C.J. Brown, J. Nielsen (eds*), Silos Fundamentals of theory, behaviour and design*, E&FN Spon, (1998) 378-399.

[11] R. Greiner, *Analysis and construction of cylindrical steel cylinders under non-axisymmetric loading* (in German), In Proc. *Wissenschaft und Praxis*, Vol. 31 FHS Biberach/Riss, Germany, (1983).